

The short running page heading

Three-dimensional morphological analysis of sacroiliac joint

Paper Title

Three-dimensional morphological analysis of the human sacroiliac joint: their influences on the degenerative changes of the auricular surfaces

Authors names

Keita Nishi^{1,2}, Toshiyuki Tsurumoto¹, Keishi Okamoto¹, Keiko Ogami¹, Takashi Hasegawa^{2,3}, Takefumi Moriuchi³, Junya Sakamoto⁴, Joichi Oyamada⁵, Toshio Higashi³, Yoshitaka Manabe⁵, Kazunobu Saiki¹

Authors affiliations

- 1 Department of Macroscopic Anatomy, Graduate School of Biomedical Science, Nagasaki University, Japan
- 2 Department of Rehabilitation, Wajinkai Hospital, Nagasaki, Japan
- 3 Department of Community-based Rehabilitation Sciences, Graduate School of Biomedical Sciences, Nagasaki University, Nagasaki, Japan
- 4 Department of Physical Therapy Science, Graduate School of Biomedical Sciences, Nagasaki University, Nagasaki, Japan
- 5 Department of Oral Anatomy and Dental Anthropology, Graduate School of Biomedical Science, Nagasaki University, Nagasaki, Japan

Abstract

The sacroiliac joint (SIJ) is responsible for weight transmission between the spine and lower extremity. However, details of the structure and function of the SIJ remain unclear. In a previous study, we devised a method of quantitatively evaluating the level of degeneration of the SIJ by using an age estimation procedure for the auricular surface of the ilium (ASI). Our results in that study suggested that the degree of degeneration of the joint surface may be associated with the morphology of the ASI. In that study, however, the morphology of the ASI was simplified for analysis, meaning that more detailed investigations were required in future. In the present study, we focused on individual differences in SIJ shape and carried out three-dimensional quantitative evaluation of the morphology of the ASI to ascertain its association with joint degeneration. We produced three-dimensional images of the right ASIs of 100 modern Japanese men (age 19–83), and obtained the three-dimensional rectangular coordinates of 11 defined measurement points. We then calculated 16 parameters indicating the morphological characteristics of the ASIs from the three-dimensional rectangular coordinates of these measurement points, and used these to perform principal component analysis to investigate trends in ASI morphology. We found that the morphology of the ASI could be characterized in terms of (i) size, (ii) concavity of the posterior border (CPB), and (iii) amount of undulation. An investigation of the correlation between these parameters and age suggested that the amount of undulation of the ASI tends to diminish with advancing age. In an investigation of the association between ASI morphology and degeneration of the articular surface, when the subjects were divided into a high-degeneration group (HDG) ($n = 55$) and a low-degeneration

group (LDG) ($n = 45$) and the 16 parameters were compared, there was a significant difference in the amount of undulation of the ASI. In an investigation limited to older subjects aged ≥ 60 ($n = 47$) at the time of death, there were significant differences between HDG ($n = 27$) and LDG ($n = 20$) in terms of not only the parameters indicating the amount of undulation of the ASI but also of those indicating the amount of CPB. These results suggested that the amount of undulation of the ASI may affect the degree of degeneration of the articular surface. In addition, in older subjects, the amount of CPB of the SIJ may also affect the degree of degeneration of the articular surface. It is thus likely that differences in ASI morphology may affect degenerative changes in the SIJ.

Keywords: sacroiliac joint; auricular surface; three-dimensional morphological analysis; morphology; degeneration

Introduction

The sacroiliac joints (SIJs) are composed of the auricular surfaces of the ilium and sacrum. Its articular surfaces are covered with irregular elevations and depressions that interlock with each other, and its mobility is extremely low (Standring 2008). In general, the auricular surface on the sacral side is concave, whereas the auricular surface on the iliac side is convex. In humans, a bipedal species, the SIJs play the role of "hubs" for transmitting force from the trunk to the ground as well as in the opposite direction (Lovejoy et al. 1985; Aiello & Dean 1990). The SIJ had to become more stable both for the coordinated movement of the pelvis itself on the femur and to enable a flexible response to the transmission of various different forces (Vleeming et al. 1990a, b; Vleeming & Stoeckart 2007). Even though the structure and function of the SIJ have been well studied, its details still remain unclear (Sashin 1930; Bowen & Cassidy 1981; Vleeming et al. 2012, 1989a, b, 1995; Pool-Goudzwaard et al. 2001; Adams & Dolan 2005; Cohen 2005; Foley & Buschbacher 2006; Forst et al. 2006).

In adults, the SIJ is generally either auricular, L-shaped, or C-shaped in form. The cranial side of the SIJ is short, and its caudal side is long. On the frontal plane, its articular surfaces are broad on the cranial side and grow narrower in the caudal direction, so that the entire articular surface is shaped like a sine wave or propeller (Solonen 1957; Bowen & Cassidy 1981; Dijkstra et al. 1989; Vleeming et al. 1990a). The articular surfaces of the SIJ have complementary comb-shaped depressions and projections on the iliac and sacral auricular surfaces that generate the highest coefficient of friction of any of the joints in the human body (Bowen & Cassidy 1981; Vleeming et al. 1990a, b). These anatomical studies precisely explain the characteristics of the SIJ as a highly

distinctive joint that is required to provide stable (and flexible) support for the human upper body. However, studies have found that the morphology of the SIJ is highly varied (Schunke 1938; Lovejoy et al. 1985), and the effect of these differences in morphology on the function of the SIJ and on individuals has gone almost unaddressed.

One characteristic of the auricular surface of the ilium (ASI) is that its morphology changes with increasing age, and this has been utilized in a proposed method of estimating age from bone specimens (Brooke 1924; Sashin 1930; Schunke 1938; MacDonald & Hunt 1952; Carter & Loewi 1962; Bowen & Cassidy 1981; Lovejoy et al. 1985; Buckberry & Chamberlain 2002; Schmitt 2004; Igarashi et al. 2005; Mulhern & Jones 2005; Nagaoka & Hirata 2008; Passalacqua 2009; Moraitis et al. 2014). In a previous study, we used this method of estimating age from the ASI to propose a method of quantitatively evaluating the degree of degenerative changes in the SIJ. In that study, we focused on the fact that there is variation in the concavity of the posterior border (CPB) of the SIJ. We carried out a two-dimensional quantitative evaluation of the CPB of the ASI, and investigated its association with degenerative changes in the SIJ. Our results suggested that for older subjects aged ≥ 60 years at the time of death, individuals with greater CPB tended to exhibit more advanced degeneration of the articular surfaces of the SIJ and hip joint (Nishi et al. 2016). However, we were concerned that this method only permitted a simple evaluation of SIJ morphology, and did not enable the assessment of the three-dimensional structure of the SIJ. In the present study, we therefore devised a comparatively easy method of quantitatively evaluating three-dimensional structure, and used this to investigate the association between the three-dimensional morphological characteristics of the SIJ and degenerative changes in the articular surface.

Subjects and Methods

Subjects

The subjects were the right ASIs of the macerated bones of 100 modern Japanese men (age range 19–83 years at the time of death) (Table 1). The subjects were restricted to men because childbirth is a major factor affecting the degree of degeneration of the articular surface in women. These bone specimens were taken from cadavers voluntarily donated to Nagasaki University School of Medicine for dissection by medical students from the 1950s to the 1970s. No identifying information other than age at death was available for the specimens used. Skeletons of patients with rheumatoid arthritis, those with lesions due to infection or other causes, those with fracture or other traumatic injury, and those in which the ASI could not be observed because of fusion of the SIJ were excluded. The measurements and investigations were performed after this study had been approved by the Ethics Committee of the Nagasaki University Graduate School of Biomedical Sciences (Department of Medicine) (approval number: 15033076). All experimental procedures were conducted in accordance with the Declaration of Helsinki.

Acquisition of three-dimensional quantitative data

Measurements were carried out by using the following method of three-dimensional quantitative evaluation of the morphology of the ASI. The right pelvic bone was first placed on a rotating scanning plate. The ASI was then photographed alongside a scale using a fixed digital camera (EOS Kiss X3, Canon, Japan) in such a way as to show the entire ASI. The scanning plate was then rotated horizontally by 15° , and the ASI was photographed again. SteroScan 3D modeling software (<http://www.agisoft.ru/products/stereoscan>, Agisoft LCC, St. Petersburg, Russia) was then used to construct a three-dimensional image from the two digital photographs, and this was then saved in PDF format as an image with three-dimensional rectangular coordinates. The measurement points were assigned on a computer screen using the three-dimensional image thus acquired by Adobe Reader XI (Adobe Systems Incorporated, San Jose, USA) (Figure 2).

Measurement procedure for parameters

The procedure for assigning measurement points first involved drawing a straight line touching the posterior border of the ASI for use as a reference line. The 11 measurement points were defined in terms of this reference line as follows (Figure 2a):

- a: Upper point of tangency of the reference line with the posterior border of the auricular surface
- b: Lower point of tangency of the reference line with the posterior border of the auricular surface
- c: Point projecting furthest anterior perpendicular to the reference line
- d: Peak of the CPB of the auricular surface

e: Point of tangency of a line perpendicular to the reference line with the superior border of the auricular surface

f: Point of tangency of a line perpendicular to the reference line with the inferior border of the auricular surface

g: Point on the anterior border on a line dropped vertically from the midpoint of “c” and “e”

h: Point on the anterior border on a line dropped vertically from the midpoint of “c” and “f”

i: Midpoint of “a” and “g”

j: Midpoint of “c” and “d”

k: Midpoint of “b” and “h”

The three-dimensional rectangular coordinates (x, y, z) of measurement points a–k were obtained on a computer monitor. The values of these coordinates were acquired in millimeters (mm) after standardization with respect to the length of the scale photographed together with the ASI.

From these three-dimensional rectangular coordinates of the 11 measurement points, we then calculated 16 parameters indicating the morphological characteristics of the SIJ. The parameters were defined as follows:

(A) Longitudinal axis of the auricular surface: Rectilinear distance between points “e” and “f”

(B) Transverse diameter of the auricular surface: Rectilinear distance from the reference line to point “c”

(C) Depth of concavity: Rectilinear distance from the reference line to point “d”

(D) Length of the short arm: Rectilinear distance between points “c” and “e”

- (E) Width of the upper part: Rectilinear distance between points “a” and “g”
- (F) Length of the long arm: Rectilinear distance between points “c” and “f”
- (G) Width of the lower part: Rectilinear distance between points “b” and “h”
- (H) Circumference of the auricular surface: Line joining points “a”, “e”, “g”, “c”, “h”, “f”, “b”, and “d”
- (I) Height of the upper part: Vertical line from point “i” to the plane defined by points “c”, “e”, and “f”
- (J) Height of the middle part: Vertical line from point “j” to the plane defined by points “c”, “e”, and “f”
- (K) Height of the lower part: Vertical line from point “k” to the plane defined by points “c”, “e”, and “f”
- (L) Angle of the anterior border: Angle formed by points “g”, “c”, and “h”
- (M) Angle of the posterior border: Angle formed by points “a”, “d”, and “b”
- (N) Area of the upper part: Sum of the areas of the upper six triangles
- (O) Area of the lower part: Sum of the areas of the lower 6 triangles
- (P) Total area: Sum of the areas of the upper and lower parts

The units used for the various parameters were millimeters (mm) for distance, degrees (°) for angles, and square millimeters (mm²) for area. The following investigations were conducted based on these measurement values (Figure 3).

Evaluation of the degree of degeneration of the ASI

The degree of degenerative changes in the ASI of the 100 specimens was assessed macroscopically. We followed the procedure used in our previous study, which is an application of the ASI-based method of estimating age reported by Buckberry &

Chamberlain (2002) and Igarashi et al. (2005) (Nishi et al. 2016). The difference between the value on the regression curve (calibrated age value, CA) calculated from the age at the time of death (AD) and the estimated age (EA) of the subjects at death according to the approximation formula

$$CA = 30.597 \times \ln(AD) - 62.553$$

CA: Calibrated age values, AD: Age at the time of death

and the estimated age was defined as the deflection of the auricular surface (DEF), a value that reflects the degree of degenerative changes in the ASI

$$DEF = EA - CA$$

DEF; Deflection of auricular surface, EA; Estimated age

In this study, specimens were divided into high-degeneration group (HDG) and low-degeneration group (LDG) according to whether their DEF values were positive or negative, and the values of the parameters calculated in the three-dimensional analysis were compared between the two groups (Figure 4).

Verification of the validity and reliability of the measurement procedure

Measurements of the right ASIs of 10 specimens were carried out to verify the validity and reliability of the measurement procedure. To verify its validity, the rectilinear distances between the measurement points were first measured with digital calipers (MITSUTOYO, Japan). The correlation between the directly measured values and the values obtained from three-dimensional imaging was then calculated by using Spearman's rank correlation coefficient. To verify its reliability, the procedure from specimen imaging to computer analysis was carried out by two different investigators,

and the intraclass correlation coefficient (ICC) between the values for the 16 parameters obtained by the two investigators was calculated.

Principal component analysis of the 16 parameters

To characterize the three-dimensional morphology of the ASI on the basis of the values of the parameters thus obtained, principal component analysis was performed using the 16 parameters for all 100 ASI specimens as continuous variables. To confirm the effect of aging on these parameters, the correlation between each of the 16 parameters and age at death was also investigated.

Association between the morphology of the ASI and the degree of degeneration of the articular surface

To investigate the association between the morphology of the ASI and degeneration of the articular surface, the specimens were divided into the HDG ($DEF \geq 0$, $n = 55$) and the LDG ($DEF < 0$, $n = 45$) on the basis of their DEF value, which indicates the degree of degenerative changes in the ASI, and differences in the values of the 16 parameters between the two groups were tested for significance.

Association between the morphology of the ASI and the degree of degeneration of the articular surface in subjects aged ≥ 60 at the time of death

To investigate the effect of the morphology of the ASI on joint degeneration in older subjects, the specimens were limited to those from subjects aged ≥ 60 at the time of death ($n = 47$) and the same comparison as above was performed between HDG (DEF ≥ 0 , $n = 27$) and LDG (DEF < 0 , $n = 20$).

Statistical analysis

All tests were carried out using JMP Pro 13.0.0 statistical software (SAS Institute Inc. North Carolina, USA). The subjects of principal component analysis were those for which the cumulative contribution ratio exceeded 80%. Parameters for which the absolute values of the factor loading coefficient exceeded 0.4 were used to interpret the results of principal component analysis. Spearman's rank correlation coefficient was used to test for correlations. Intergroup comparisons were performed using either an unpaired t-test or Mann-Whitney U test after the data for the various parameters had been tested for normality. The significance level was set at $\leq 5\%$.

Results

Verification of the validity and reliability of the measurement procedure

There was an extremely strong positive correlation between the directly measured values and those obtained from the three-dimensional images ($r = 0.991$, $p < 0.001$). A

comparison of the values measured by different investigators found that ICC (2,1) was 0.990 (95% confidence interval: 0.984–0.993), indicating high reproducibility.

Principal component analysis of 16 parameters

Principal component analysis using the 16 parameters indicating the three-dimensional morphology of the ASI as variates found that the cumulative contribution ratio up to the 5th principal component was 81.251%, and the components up to the 5th principal component were therefore used as the subjects of analysis (Table 2).

In the first principal component, factor loading that can be regarded as indicating the overall size of the ASI, such as the circumference of the auricular surface (H), the area of the upper part (N), the area of the lower part (O), the total area (P), the longitudinal axis of the auricular surface (A), length of the short arm (D), and length of the long arm (F), as well as the transverse diameter of the auricular surface (B), the width of the upper part (E), and the width of the lower part (G), were large, and all had positive values.

In the second principal component, the absolute values of the depth of concavity (C) and the angle of the posterior border (M), which indicate the degree of CPB of the ASI, were large. The value of factor loading for the depth of concavity was positive, but that of the angle of the posterior border was negative.

In the third principal component, the absolute values of the factor loading of the height of the upper part (I), the height of the middle part (J), and the height of the lower

part (K) were large. The factor loading of the heights of the upper, middle, and lower parts all had positive values.

In the fourth principal component, the overall values for the factor loading of the area of the upper part (N) and the width of the upper part (E), which indicate the size of the short arm of the auricular surface (the upper articular surface of the auricular surface), were large. The factor loading for the area and width of the upper part had positive values.

In the fifth principal component, the absolute values of the factor loading for the angle of the anterior border (L) and the longitudinal axis of the auricular surface (A), which indicate the size of the auricular surface in the craniocaudal direction, were large. The factor loading for both the angle of the anterior border and the longitudinal axis of the auricular surface both had positive values (Table 3).

The correlation analysis performed to investigate the association between the various parameters and aging revealed significant negative correlations with the height of the upper part (I) ($r = -0.286$, $p = 0.004$), the height of the middle part (J) ($r = -0.239$, $p < 0.017$), and the height of the lower part (K) ($r = -0.309$, $p = 0.002$). The heights of the upper, middle, and lower parts thus tended to decrease with advancing age (Table 4).

Association between the morphology of the ASI and the degree of degeneration of the articular surface

In the comparison between HDG and LDG including all 100 specimens, the only significant difference was for the height of the middle part (J) (HDG: 1.77 ± 1.45 ; LDG:

2.21 ± 1.14 ; $p = 0.012$). The height of the middle part was thus significantly higher in the LDG than in the HDG (Figure 5).

Association between the morphology of the ASI and the degree of degeneration of the articular surface in subjects aged ≥ 60 at the time of death

In the comparison between HDG and LDG including 47 samples from subjects aged ≥ 60 at the time of death, there were significant differences in the depth of concavity (C) (HDG: 11.29 ± 3.69 ; LDG: 8.90 ± 2.72 ; $p = 0.019$), the angle of the posterior border (M) (HDG: 122.35 ± 14.47 ; LDG: 131.91 ± 12.38 ; $p = 0.022$), the height of the middle part (J) (HDG: 1.39 ± 0.90 ; LDG: 2.11 ± 0.95 ; $p = 0.013$), and the height of the lower part (K) (HDG: 1.27 ± 0.97 ; LDG: 2.34 ± 1.62 ; $p = 0.045$). The depth of concavity was significantly greater in the HDG than in the LDG, and the angle of the posterior border was significantly greater in the LDG than in the HDG. The heights of both the middle and lower parts were significantly higher in the LDG than in the HDG (Figure 6).

Discussion

Method of measuring the three-dimensional morphology of the ASI used in this study

Thanks to recent dramatic advances in image analysis technology, numerous studies are now using computed tomography or magnetic resonance imaging to carry out three-dimensional analysis of the skeletal structure of the human body. Data acquisition

for the three-dimensional analysis procedure used in this study is comparatively easy, enabling three-dimensional images to be obtained from two digital photographs taken at different angles. There was an extremely strong positive correlation between the data from the three-dimensional images produced by this procedure and macroscopically measured values, indicating that this method of measurement has high validity. In the study of inter-investigator reliability, ICC (2,1) was 0.990, demonstrating high reproducibility. These findings suggested that the method of three-dimensional analysis we used in this study, which does not require specialized measurement apparatus or scanning devices, provides accurate data extremely cheaply and easily, and may be useful for future three-dimensional studies.

Characteristics of the three-dimensional morphology of the ASI

In an anatomical study of the bones of the SIJ in men, Schunke reported that there is considerable individual variation in size, shape, and circumference (Schunke 1938). In our previous study of the two-dimensional morphology of the ASI, we also found wide variation between individuals in the shape of the ASI, which could be L-shaped, C-shaped, or elliptical, among other possibilities (Nishi et al. 2016).

This is the first full-scale study to attempt to quantify the three-dimensional morphological characteristics of the ASI. We found that it can be characterized in terms of (i) size, (ii) CPB, and (iii) amount of undulation. In a study of the changes in the surface of the human ilium from birth to adolescence, Yusof et al. found that the surface area of the ASI increased rapidly from soon after birth until around 4 years of age. This period overlaps with the stage of human development in which children progress from a

supine, non-weight-bearing environment to becoming capable of walking on two legs, and Yusof et al. suggest that the structure of the ASI may thus change in preparation for bipedalism and to maintain it (Yusof et al. 2013). The fact that in this study the parameters indicating the size of the ASI and the amount of CPB were not correlated with age may have been because the samples were from subjects older than adolescence at the time of death. This suggests that the size and CPB of the ASI may thus undergo morphological changes for several years after birth as a result of mechanical factors such as weight-bearing stress on the SIJ but that their morphology does not change greatly after adolescence.

In terms of the undulation of the ASI, numerous studies using the ASI as a method of estimating age have reported that the articular surface becomes flatter with age (Brooke 1924; Sashin 1930; Schunke 1938; MacDonald & Hunt 1952; Carter & Loewi 1962; Bowen & Cassidy 1981; Lovejoy et al. 1985; Buckberry & Chamberlain 2002; Schmitt 2004; Igarashi et al. 2005; Mulhern & Jones 2005; Nagaoka & Hirata 2008; Passalacqua 2009; Moraitis et al. 2014). However, these studies all looked at the articular cartilage of the auricular surface and its surface properties, rather than the undulation of the articular surface as a whole measured in the present study. To our knowledge, ours is the first study to quantitatively evaluate the measured heights of protuberances in three dimensions and isolate them as morphological characteristics of the ASI. We found that the amount of undulation of the ASI tends to diminish with advancing age. This result suggested that in addition to flattening of the articular surface, age-related changes in the ASI also include flattening of the undulation of the articular surface as a whole.

Association between the morphology of the ASI and the degree of degeneration of the articular surface

In this study, we calculated the deflection of the auricular surface (DEF), a value that indicates the degree of degeneration of the ASI, from the calibrated age (CA) values derived from the regression curve of age at the time of death (AD) and estimated age (EA). The regression curve was used because the estimated age may be underestimated in specimens from subjects who died at a young age. We thus attempted to resolve this problem by using an exponential curve. As a result, there was a strong correlation between AD and EA ($r = 0.857$), increasing the validity of the DEF in young subjects.

In the comparison of the various parameters between the HDG and LDG when all the subjects were included, we found that the height of the middle part was significantly greater in the LDG than in the HDG. The heights of the upper and lower parts also tended to be greater, although these differences were not statistically significant. A number of studies that have used computed tomography to investigate differences in the joint space of the SIJ at different ages have found that the joint space narrows with increasing age (Vogler et al. 1984; Shibata et al. 2002; Demir et al. 2007). Shibata et al. also reported that this degeneration of the SIJ may begin as early as post-pubertal adolescence (Shibata et al. 2002). Because the SIJ is located in the pelvis, the stability of which is key to bipedalism in humans, it is constantly subject to weight-bearing stress. The level of this mechanical stress also varies according to individual lifestyles (such as manual work or intellectual work). One limitation of the present study was that we were unable to gather any information on the backgrounds of the subjects while they were alive. However, our results did suggest that a decrease in the height of the protuberances

on the ASI was associated with the progression of degenerative changes in the ASI, and this effect may begin from adolescence.

The effect of the morphology of the ASI on joint degeneration was expected to be more obvious in older subjects than in younger ones. We therefore carried out an investigation limited to samples from older subjects aged ≥ 60 at the time of death. We found that not only the heights of the middle and lower parts, but also the depth of concavity and the angle of the posterior border differed significantly between the HDG and the LDG. The depth of concavity and the angle of the posterior border are parameters indicating the amount of CPB of the ASI. In our previous study, we carried out a quantitative evaluation of the CPB of the ASI in two dimensions, and found that in older subjects, individuals with larger CPB exhibited a greater degree of joint degeneration compared with individuals with smaller CPB (Nishi et al. 2016). The depth of concavity and the angle of the posterior border were only weakly correlated with age, suggesting that the amount of CPB of the ASI may not change after a certain age (possibly after puberty). Our results in the present study suggested that the CPB of the ASI may have little effect on the degeneration of the articular surface during the period from early to late middle age, but that it may have an effect from old age onward. The joint movement of the SIJ is generally considered to involve the anteroposterior rotation of the sacrum with respect to the ilium in the sagittal plane (Weisl 1955; Kapandji 2008). The extent of anteroposterior rotation of the SIJ may thus be greater in individuals with a large CPB of the ASI compared with those in whom it is smaller. The amount of CPB of the ASI may thus be associated with the extent of mobility of the SIJ. Because the stability of the SIJ is absolutely essential in bipedal humans, as mentioned above, in individuals in whom it has a greater range of movement, this stability may be

derived from the tensile force of the muscles and fascia around the SIJ. With advancing age, however, increasing muscle weakness makes the maintenance of joint stability by means of the tensile strength of muscles or fascia more difficult, which may increase the mechanical stress imposed on the tendons at the joint margins and on the articular surface. Vleeming et al. reported that impairment of the stability mechanisms of the SIJ may lead to degenerative damage to the joint, resulting in clinical symptoms of pelvic girdle pain (Vleeming et al. 2012). Our own findings suggested that individuals with a larger CPB of the ASI may have difficulty in maintaining the stability mechanisms of the SIJ as they become older.

Among the limitations of this study were the wide variation in the ages of the subjects at death, and particularly the small number of adolescent subjects. In future studies, the number of subjects in each age group should be adjusted to investigate age-related changes in morphology. Increasing the number of subjects and restricting them to members of specific age groups may also help to elucidate the association between the morphology of the ASI and degenerative changes to the joint in greater detail. Because the subjects of this study were bone specimens, it was not possible to ascertain their living environments or whether they had experienced problems with the SIJ during life. However, we were successful in identifying the three-dimensional morphological characteristics of the ASI and in investigating the association between this morphology and degeneration of the articular surface, which may prove helpful in improving our understanding of the functional anatomy of the SIJ and its kinematics.

In conclusion, the morphology of the ASI could be characterized in terms of the size of the joint surface, its CPB, and the amount of undulation. Our results also suggested that the amount of undulation of the ASI tended to diminish with advancing age. An

investigation of the association between the morphology of the ASI and degeneration of the articular surface found that the amount of undulation may affect the degree of degeneration of the articular surface. Our results also suggested that in older subjects, the amount of CPB of the SIJ may affect the degree of degeneration of the articular surface. These results indicate that it is likely that variations in the morphology of the ASI may affect degenerative changes in the SIJ.

Acknowledgements

We would like to thank Dr. Katsutomo Kato for leading our study. We would like to thank the members of macroscopic anatomy laboratory of Nagasaki University that provided the specimens and the members of Community-based Rehabilitation Sciences Laboratory of Nagasaki University who gave valuable suggestions in this research.

Author contributions

Concept/design: K.N., K.S., T.T. Acquisition of data: K.N., K.S. Data analysis/interpretation: K.N., K.S., K.O., K.T., T.H., T.M., J.S., J.O., T.H., Y.M., T. T. drafting of the manuscript: K.N., K.S., T.T.

References

- Adams MA, Dolan P (2005) Spine biomechanics. *J Biomech* 38, 1972–1983.
- Aiello LC, Dean C (1990) Bipedal locomotion and the postcranial skeleton. In: *An Introduction to Human Evolutionary Anatomy*. Elsevier Science Publishing Co. Inc, San Diego; pp 244–274.

- Bowen V, Cassidy J (1981) Macroscopic and microscopic anatomy of the sacroiliac joint from embryonic life to the the eighth decade. *Spine* (Phila Pa 1976) 6, 620–628.
- Brooke R (1924) The sacro-iliac joint. *J Anat* 58, 299–305.
- Buckberry JL, Chamberlain AT (2002) Age estimation from the auricular surface of the ilium: A revised method. *Am J Phys Anthropol* 119, 231–239.
- Carter M, Loewi G (1962) Anatomical changes in normal sacroiliac joints during childhood and comparison with the changes in Still's disease. *Ann Rheum Dis* 21, 121–134.
- Cohen SP (2005) Sacroiliac joint pain: A comprehensive review of anatomy, diagnosis and treatment. *Anesth Analg* 101,1440–1453.
- Demir M, Mavi A, Gümüşburun E, et al. (2007) Anatomical variations with joint space measurements on CT. *Kobe J Med Sci* 53, 209–217.
- Dijkstra PF, Vleeming A, Stoeckart R (1989) Complex motion tomography of the sacroiliac joint. An anatomical and roentgenological study. *Rofo* 150, 635–642.
- Foley BS, Buschbacher RM (2006) Sacroiliac joint pain: anatomy, biomechanics, diagnosis, and treatment. *Am J Phys Med Rehabil* 85, 997–1006.
- Forst SL, Wheeler MT, Fortin JD, et al. (2006) The sacroiliac joint: anatomy, physiology and clinical significance. *Pain Physician* 9, 61–67.
- Igarashi Y, Uesu K, Wakebe T, et al. (2005) New method for estimation of adult skeletal age at death from the morphology of the auricular surface of the ilium. *Am J Phys Anthropol* 128, 324–339.
- Kapandji IA (2008) *The Physiology of the Joints*, volume III, 6th edn. Churchill Livingstone, Edinburgh, Scotland

- Lovejoy CO, Meindl RS, Pryzbeck TR, et al. (1985) Chronological metamorphosis of the auricular surface of the ilium: A new method for the determination of adult skeletal age at death. *Am J Phys Anthropol* 68, 15–28.
- MacDonald GR, Hunt TE (1952) Sacroiliac joints: Observations on the gross histological changes in the various age groups. *Can Med Assoc J* 66, 157–163.
- Moraitis K, Zorba E, Eliopoulos C, et al. (2014) A test of the revised auricular surface aging method on a modern European population. *J Forensic Sci* 59, 188–194.
- Mulhern D, Jones E (2005) Test of revised method of age estimation from the auricular surface of the ilium. *Am J Phys Anthropol* 126, 61–65.
- Nagaoka T, Hirata K (2008) Demographic structure of skeletal populations in historic Japan: a new estimation of adult age-at-death distributions based on the auricular surface of the ilium. *J Archaeol Sci* 35, 1370–1377.
- Nishi K, Saiki K, Imamura T, et al (2016) Degenerative changes of the sacroiliac auricular joint surface—validation of influential factors. *Anat Sci Int* 1–9.
- Passalacqua NV. (2009) Forensic age-at-death estimation from the human sacrum. *J Forensic Sci* 255–262
- Pool-Goudzwaard AL, Kleinrensink GJ, Snijders CJ, et al (2001) The sacroiliac part of the iliolumbar ligament. *J Anat* 199, 457–463.
- Sashin D (1930) A critical analysis of the anatomy and the pathological changes of the sacroiliac joints. *J Bone Jt Surg* 12, 891–910.
- Schmitt A (2004) Age-at-death assessment using the os pubis and the auricular surface of the ilium: A test on an identified Asian sample. *Int J Osteoarchaeol* 14, 1–6.
- Schunke G (1938) The anatomy and development of the sacroiliac joint in man. *Anat Rec* 72, 313–331.

- Shibata Y, Shirai Y, Miyamoto M (2002) The aging process in the sacroiliac joint: helical computed tomography analysis. *J Orthop Sci* 7, 12–18.
- Solonen K (1957) The sacroiliac joint in the light of anatomical, roentgenological and clinical studies. *Acta Orthop Scand* 28(Suppl), 1–127.
- Standring S (2008) Gray's Anatomy, 40th edn. Churchill Livingstone, Edinburgh, Scotland
- Vleeming A, Pool-Goudzwaard AL, Stoeckart R, et al (1995) The posterior layer of the thoracolumbar fascia. Its function in load transfer from spine to legs. *Spine* (Phila Pa 1976) 20, 753–8.
- Vleeming A, Schuenke MD, Masi AT, et al (2012) The sacroiliac joint: an overview of its anatomy, function and potential clinical implications. *J Anat* 221, 537–567.
- Vleeming A, Stoeckart R (2007) The role of the pelvic girdle in coupling the spine and the legs: a cinical-anatomical perspective on pelvic stability. In: Vleeming A, Mooney V, Stoeckart R (eds) *Movement, Stability and Lumbopelvic Pain: Integration and Research*. Churchill Livingstone, Edinburgh, Scotland, pp 113–137
- Vleeming A, Stoeckart R, Snijders CJ (1989a) The sacrotuberous ligament: a conceptual approach to its dynamic role in stabilizing the sacroiliac joint. *Clin Biomech* 4, 201–203.
- Vleeming A, Stoeckart R, Volkers AC, et al. (1990a) Relation between form and function in the sacroiliac joint. Part I: Clinical anatomical aspects. *Spine* (Phila Pa 1976) 15, 130–132.

- Vleeming A, Van Wingerden JP, Snijders CJ, et al. (1989b) Load application to the sacrotuberous ligament; influences on sacroiliac joint mechanics. *Clin Biomech* 4, 204–209.
- Vleeming A, Volkers A, Snijders C, et al. (1990b) Relation between form and function in the sacroiliac joint. Part II: Biomechanical aspects. *Spine* (Phila. Pa. 1976) 15, 133–136.
- Vogler JB, Brown WH, Helms CA, et al. (1984) The normal sacroiliac joint: a CT study of asymptomatic patients. *Radiology* 151, 433–7.
- Weisl H (1955) Movements of the sacroiliac joint. *Acta Anat* (Basel) 23, 80–91.
- Yusof NA, Soames RW, Cunningham CA, et al. (2013) Growth of the Human Ilium: The Anomalous Sacroiliac Junction. *Anat Rec* 296, 1688–1694.

Table and figure legends

Table 1. Distribution of age at the time of death the specimens.

Table 2. Contribution ratios and cumulative contribution ratios for each principal component.

Since the cumulative contribution ratio exceeded 80% at the fifth principal component, the first through the fifth principal components (above the broken line) were used for analysis.

Table 3. Factor loading coefficients of each principal component.

The bold numbers in oblique type indicate factor loading exceeding 0.4.

Table 4. Association between the different parameters and age at the time of death.

*: $p < 0.05$

Figure 1. A, B, and C illustrate the three-dimensional measurement procedure.

A: The auricular surface of the ilium was photographed with a fixed digital camera from a distance of 70 cm, then rotated 15° in the horizontal plane and photographed again. B: The two digital photographs (JPEG format). These two images were processed using three-dimensional image production software to produce a three-dimensional image. C: The image thus produced. This image can be rotated and viewed from any angle. The images were stored in PDF format.

Figure 2. The assigned measurement points on the auricular surface.

A straight line was drawn tangential to the posterior border of the auricular surface for use as a reference line. The upper point of tangency was defined as “a”, and the lower point of tangency as “b”. The point projecting furthest anterior perpendicular to the reference line was defined as “c”, the point on the posterior border of the joint that was furthest from the reference line as “d”, the point of tangency of the perpendicular line with the superior border as “e”, and the point of tangency with the inferior border as “f”. Point “g” was defined as the point on the anterior border on a line dropped vertically from the midpoint of “c” and “e”, and similarly “h” was defined as the point on the anterior border on a line dropped vertically from the midpoint of “c” and “f”. Points “i”, “j”, and “k” were defined as the points on the auricular surface onto which lines were dropped from the midpoints of “a” and “g”, “c” and “d”, and “b” and “h”, respectively.

Figure 3. Sixteen measured parameters indicating the morphology of the auricular surface.

I: (A) Longitudinal axis of the auricular surface: Rectilinear distance between points “e” and “f”. (D) Length of the short arm: Rectilinear distance between points “c” and “e”. (E) Width of the upper part: Rectilinear distance between points “a” and “g”. (F) Length of the long arm: Rectilinear distance between points “c” and “f”. (G) Width of the lower part: Rectilinear distance between points “b” and “h”. II: (B) Transverse diameter of the auricular surface: Rectilinear distance from the reference line to point “c”. (C) Depth of concavity: Rectilinear distance from the reference line to point “d”. III: (H) Circumference of the auricular surface: Line joining points “a”, “e”, “g”, “c”, “h”, “f”, “b”, and “d”. IV: (I) Height of the upper part: Vertical line from point “I” to the plane defined by points “c”, “e”, and “f”. (J) Height of the middle part: Vertical line from point j to the plane defined by points “c”, “e”, and “f”. (K) Height of the lower part: Vertical line from point “k” to the plane defined by points “c”, “e”, and “f”. V: (L) Angle of the anterior border: Angle formed by points “g”, “c”, and “h”. (M) Angle of the posterior border: Angle formed by points “a”, “d”, and “b”. VI: (N) Area of the upper part: Sum of the areas of the six triangles above the broken line linking points “c” and “d”. (O) Area of the lower part: Sum of the areas of the six triangles below the broken line. (P) Total area: Sum of (N) and (O). Units: length in millimeters (mm) angles in degrees ($^{\circ}$), area in square millimeters (mm^2).

Figure 4. Association between age at the time of death and estimated age.

The horizontal axis shows the age at the time of death (AD) and the vertical axis the estimated age (EA) at death. The values on the regression curve, which were obtained from the AD and the EA, were defined as the calibrated age (CA) values. Subjects for whom the difference between the EA and CA was a positive value were assigned to the high-degeneration group (HDG), and those for whom it was a negative value to the low-degeneration group (LDG).

Figure 5. Box-and-whisker plot of the 16 parameters for all subjects.

The blue boxes represent the values for the low-degeneration group, and the orange boxes those for the high-degeneration group. The height of the middle part (J) differed significantly between the high-degeneration group (HDG) and low-degeneration group (LDG). *: $p < 0.05$.

Figure 6. Box-and-whisker plot of the 16 parameters for subjects aged ≥ 60 at the time of death.

The blue boxes represent the values for the low-degeneration group (LDG), and the orange boxes those for the high-degeneration group (HDG). The depth of concavity (C), the height of the middle part (J), the height of the lower part (K), and the angle of the posterior border (M) differed significantly between the HDG and LDG. *: $p < 0.05$.

Age at the time of death	Number
10 - 19	1
20 - 29	7
30 - 39	5
40 - 49	20
50 - 59	20
60 - 69	28
70 - 79	18
80 - 89	1
Total	100

Table 1. Distribution of age at the time of death the specimens.

134x131mm (300 x 300 DPI)

Ani

PC	Contribution ratios (%)	Cumulative contribution ratios (%)
1	39.303	39.303
2	13.779	53.082
3	12.148	65.230
4	8.410	73.640
5	7.611	81.251
6	6.039	87.290
7	3.247	90.564
8	2.703	93.267
9	2.648	95.914
10	1.972	97.886
11	0.938	98.824
12	0.562	99.386
13	0.353	99.740
14	0.200	99.940
15	0.060	100.000

Table 2. Contribution ratios and cumulative contribution ratios for each principal component. Since the cumulative contribution ratio exceeded 80% at the fifth principal component, the first through the fifth principal components (above the broken line) were used for analysis.

166x152mm (300 x 300 DPI)

only

Measurement parameters	PC1	PC2	PC3	PC4	PC5
(A) Longitudinal axis of auricular surface	0.768	-0.097	-0.058	-0.111	0.528
(B) Transverse diameter of auricular surface	0.901	0.002	-0.128	0.113	-0.306
(C) Depth of concavity	0.308	0.888	-0.219	-0.152	0.016
(D) Length of the short arm	0.714	0.120	-0.303	0.112	-0.294
(E) Width of upper part	0.520	0.382	0.331	0.453	0.072
(F) Length of the long arm	0.681	-0.353	-0.144	-0.236	0.269
(G) Width of lower part	0.779	-0.077	-0.044	-0.086	-0.048
(H) Circumference of auricular surface	0.929	0.220	-0.069	-0.079	0.214
(I) Height of upper part	0.140	0.267	0.771	-0.214	0.122
(J) Height of middle part	0.241	-0.105	0.718	-0.040	-0.248
(K) Height of lower part	0.224	-0.025	0.619	-0.419	-0.282
(L) Angle of anterior border	-0.464	0.303	0.287	0.223	0.651
(M) Angle of posterior border	-0.162	-0.876	0.141	0.262	0.131
(N) Area of upper part	0.571	0.002	0.197	0.701	-0.087
(O) Area of lower part	0.741	-0.285	-0.020	-0.375	0.161
(P) Total area	0.912	-0.204	0.116	0.192	0.059

Table 3. Factor loading coefficients of each principal component. The bold numbers in oblique type indicate factor loading exceeding 0.4.

112x61mm (300 x 300 DPI)

Review Only

Measurement parameters	r-value	p-value
(A) Longitudinal axis of auricular surface	0.124	0.218
(B) Transverse diameter of auricular surface	-0.060	0.557
(C) Depth of concavity	-0.112	0.269
(D) Length of the short arm	-0.026	0.796
(E) Width of upper part	-0.135	0.180
(F) Length of the long arm	0.073	0.468
(G) Width of lower part	-0.052	0.610
(H) Circumference of auricular surface	-0.031	0.761
(I) Height of upper part	-0.286	0.004*
(J) Height of middle part	-0.239	0.017*
(K) Height of lower part	-0.309	0.002*
(L) Angle of anterior border	0.081	0.422
(M) Angle of posterior border	0.144	0.154
(N) Area of upper part	-0.136	0.178
(O) Area of lower part	-0.079	0.435
(P) Total area	-0.087	0.392

Table 4. Association between the different parameters and age at the time of death.

*: $p < 0.05$

167x136mm (300 x 300 DPI)

View Only

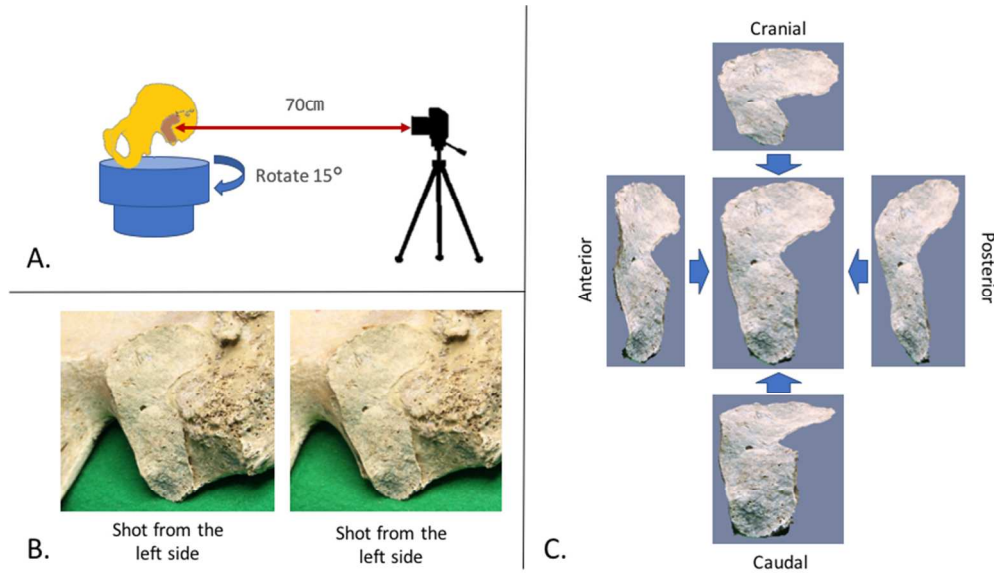


Figure 1. A, B, and C illustrate the three-dimensional measurement procedure. A: The auricular surface of the ilium was photographed with a fixed digital camera from a distance of 70 cm, then rotated 15° in the horizontal plane and photographed again. B: The two digital photographs (JPEG format). These two images were processed using three-dimensional image production software to produce a three-dimensional image. C: The image thus produced. This image can be rotated and viewed from any angle. The images were stored in PDF format.

76x44mm (300 x 300 DPI)

View Only

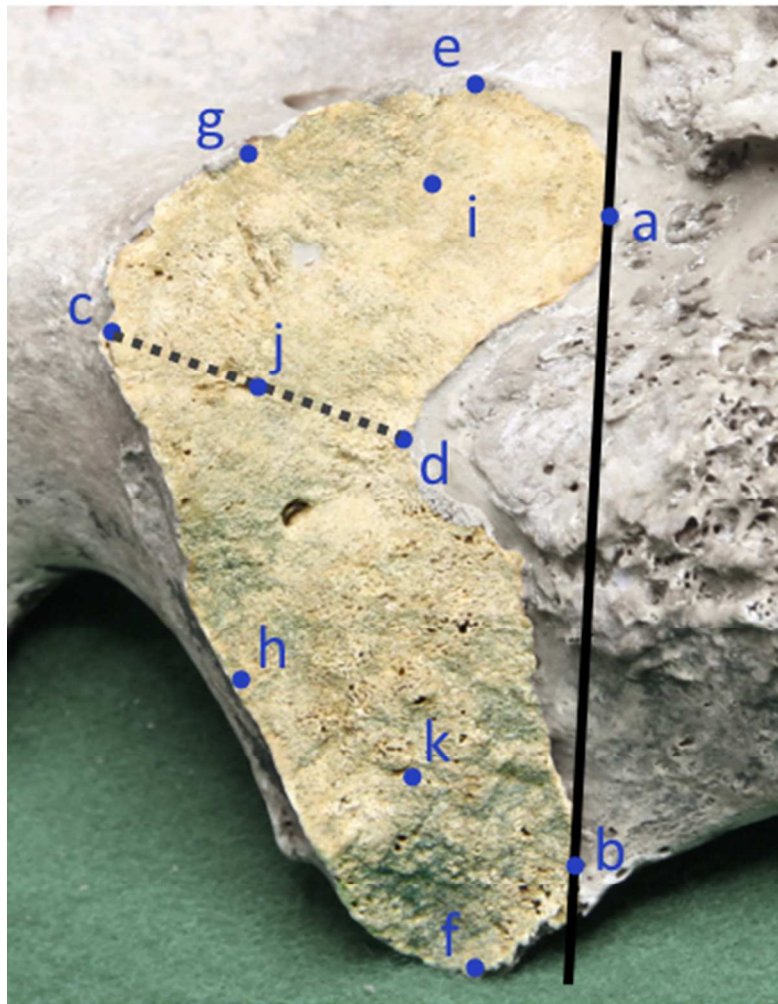


Figure 2. The assigned measurement points on the auricular surface.

A straight line was drawn tangential to the posterior border of the auricular surface for use as a reference line. The upper point of tangency was defined as "a", and the lower point of tangency as "b". The point projecting furthest anterior perpendicular to the reference line was defined as "c", the point on the posterior border of the joint that was furthest from the reference line as "d", the point of tangency of the perpendicular line with the superior border as "e", and the point of tangency with the inferior border as "f". Point "g" was defined as the point on the anterior border on a line dropped vertically from the midpoint of "c" and "e", and similarly "h" was defined as the point on the anterior border on a line dropped vertically from the midpoint of "c" and "f". Points "i", "j", and "k" were defined as the points on the auricular surface onto which lines were dropped from the midpoints of "a" and "g", "c" and "d", and "b" and "h", respectively.

33x43mm (300 x 300 DPI)

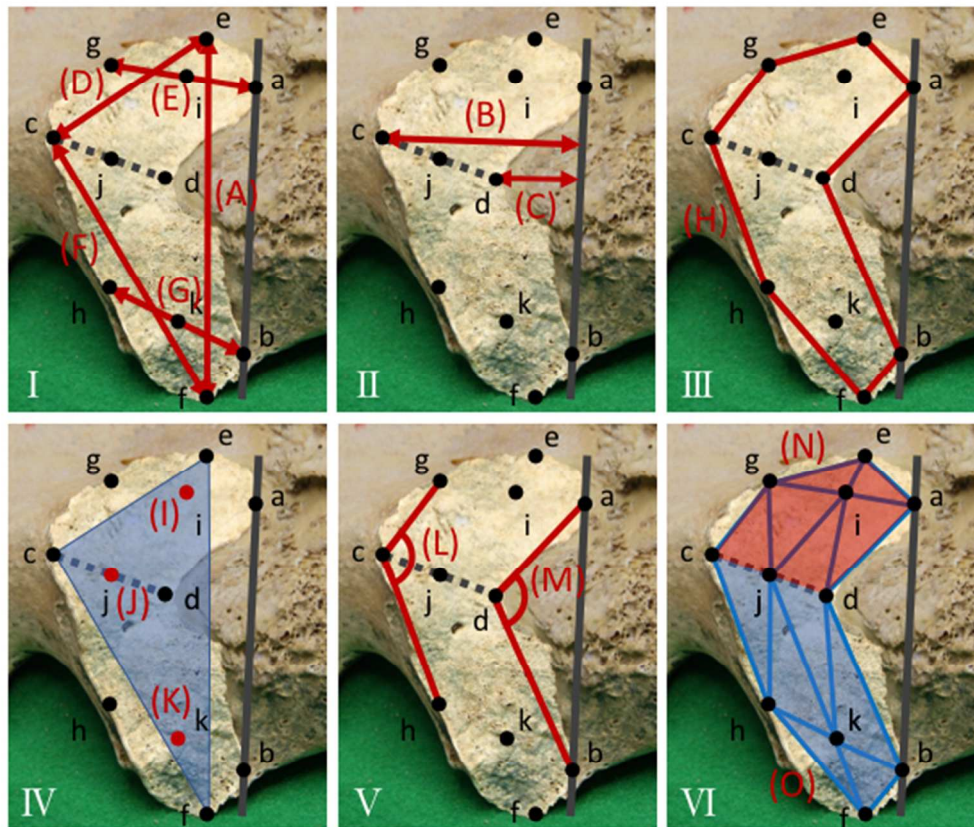


Figure 3. Sixteen measured parameters indicating the morphology of the auricular surface. I: (A) Longitudinal axis of the auricular surface: Rectilinear distance between points "e" and "f". (D) Length of the short arm: Rectilinear distance between points "c" and "e". (E) Width of the upper part: Rectilinear distance between points "a" and "g". (F) Length of the long arm: Rectilinear distance between points "c" and "f". (G) Width of the lower part: Rectilinear distance between points "b" and "h". II: (B) Transverse diameter of the auricular surface: Rectilinear distance from the reference line to point "c". (C) Depth of concavity: Rectilinear distance from the reference line to point "d". III: (H) Circumference of the auricular surface: Line joining points "a", "e", "g", "c", "h", "f", "b", and "d". IV: (I) Height of the upper part: Vertical line from point "I" to the plane defined by points "c", "e", and "f". (J) Height of the middle part: Vertical line from point "j" to the plane defined by points "c", "e", and "f". (K) Height of the lower part: Vertical line from point "k" to the plane defined by points "c", "e", and "f". V: (L) Angle of the anterior border: Angle formed by points "g", "c", and "h". (M) Angle of the posterior border: Angle formed by points "a", "d", and "b". VI: (N) Area of the upper part: Sum of the areas of the six triangles above the broken line linking points "c" and "d". (O) Area of the lower part: Sum of the areas of the six triangles below the broken line. (P) Total area: Sum of (N) and (O). Units: length in millimeters (mm) angles in degrees ($^{\circ}$), area in square millimeters (mm^2).

52x45mm (300 x 300 DPI)

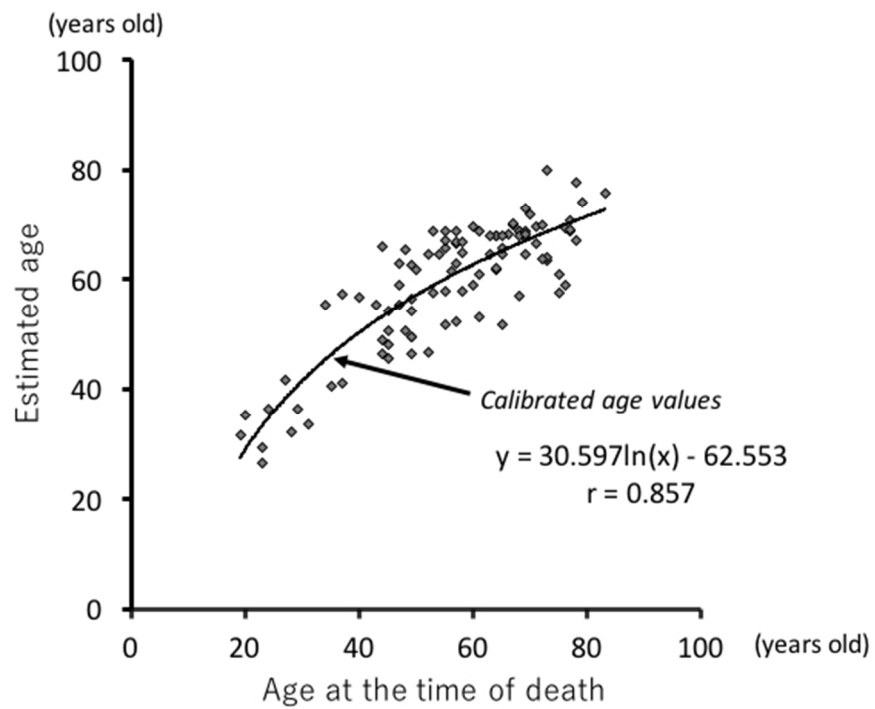


Figure 4. Association between age at the time of death and estimated age. The horizontal axis shows the age at the time of death (AD) and the vertical axis the estimated age (EA) at death. The values on the regression curve, which were obtained from the AD and the EA, were defined as the calibrated age (CA) values. Subjects for whom the difference between the EA and CA was a positive value were assigned to the high-degeneration group (HDG), and those for whom it was a negative value to the low-degeneration group (LDG).

55x40mm (300 x 300 DPI)

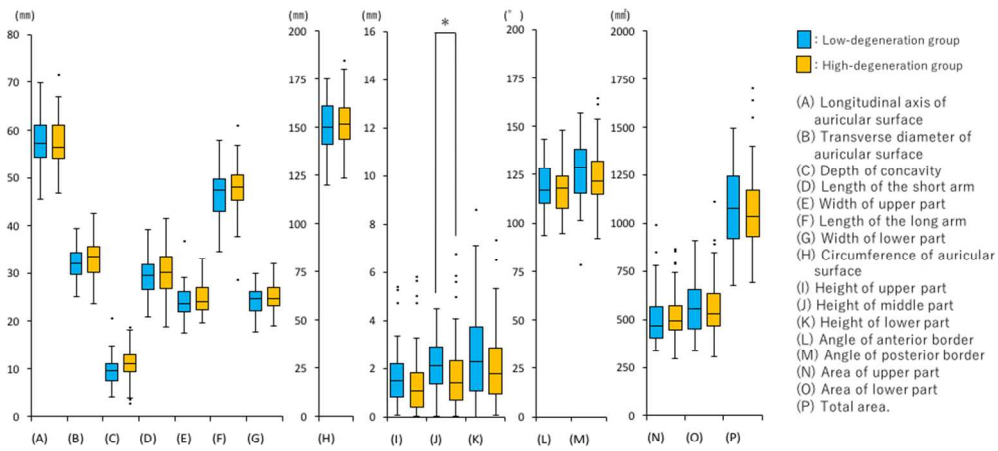


Figure 5. Box-and-whisker plot of the 16 parameters for all subjects.†
 The blue boxes represent the values for the low-degeneration group, and the orange boxes those for the high-degeneration group. The height of the middle part (J) differed significantly between the high-degeneration group (HDG) and low-degeneration group (LDG). *: $p < 0.05$.

84x45mm (300 x 300 DPI)

Review Only

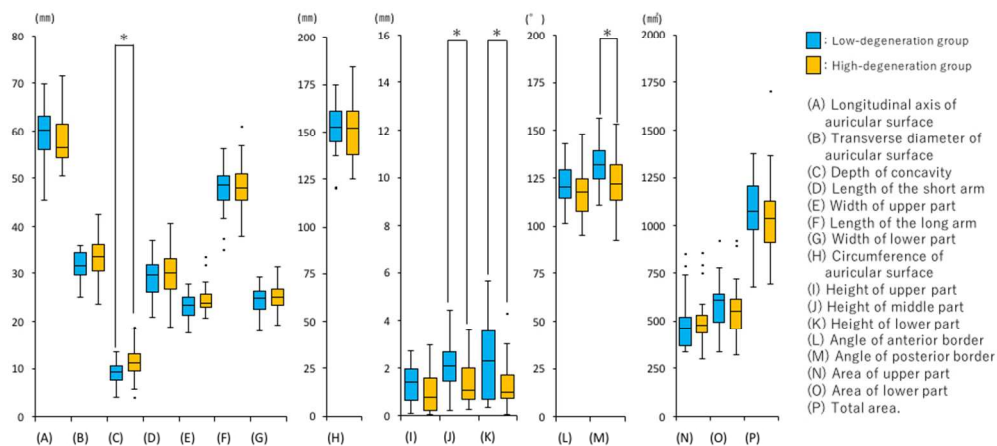


Figure 6. Box-and-whisker plot of the 16 parameters for subjects aged 60 at the time of death.[†] The blue boxes represent the values for the low-degeneration group (LDG), and the orange boxes those for the high-degeneration group (HDG). The depth of concavity (C), the height of the middle part (J), the height of the lower part (K), and the angle of the posterior border (M) differed significantly between the HDG and LDG. *: $p < 0.05$.

84x49mm (300 x 300 DPI)